DEEP-SEA RESEARCH
Part II

Deep-Sea Research II 51 (2004) 2023–2039

www.elsevier.com/locate/dsr2

Winter sea-ice properties in Marguerite Bay, Antarctica

D.K. Perovich[a,*], B.C. Elder[a], K.J. Claffey[a], S. Stammerjohn[b], R. Smith[c], S.F. Ackley[d], H.R. Krouse[e], A.J. Gow[a]

[a] *US Army Engineer Research and Development Center, Cold Regions Research and Engineering Laboratory, 72 Lyme Road, Hanover, NH 03755-1290, USA*

[b] *Lamont–Doherty Earth Observatory, Columbia University, 61 Route 9W, Palisades, NY 10964, USA*

[c] *Geography Department, University of California, Santa Barbara, Santa Barbara, CA 93106-4060, USA*

[d] *Civil and Environmental Engineering Department, Clarkson University, Potsdam, NY 13699, USA*

[e] *Physics and Astronomy Department, University of Calgary, Calgary, Alta, Canada T2N 1N4*

Accepted 11 July 2004

Abstract

During the winter 2001 and 2002 cruises of the SO-GLOBEC experiment, we investigated the morphological properties, growth processes, and internal permeability of sea ice in the Marguerite Bay area of the Western Antarctic Peninsula. There was considerable interannual variability in ice thickness with, average values of 62 cm in 2001 and 102 cm in 2002, with medians of 43 and 68 cm, respectively. Snow depth averaged 16 cm in 2001 and 21 cm in 2002. At 40% of the thickness holes in 2001 and 17% in 2002, a combination of deep snow and thin ice resulted in negative freeboard and the potential for surface flooding. Ice production was strongly influenced by the snow cover. Deep snow resulted in negative freeboard, surface flooding, and the formation of snow–ice, but also limited columnar ice growth on the bottom of the ice. A stratigraphic analysis of ice thin sections showed that more than half of the ice sampled was granular and that virtually all of the upper 20 cm of the ice cover was granular. Stable isotope ($\delta^{18}O$) analysis of samples from 2001 indicated that snow–ice formation at the surface contributed significantly to ice formation. Two-thirds of the cores had some snow–ice and 15% of the ice sampled in 2001 was snow–ice. For 95% of the ice sampled the combination of warm ice temperatures and large salinities resulted in brine volumes that were greater than the percolation threshold of 5%. Autonomous mass balance buoys indicated that the ice was above the percolation threshold throughout late winter and spring. The exceeding of the percolation threshold allows continuous flooding to occur throughout the late winter–spring period. The WAP sea-ice therefore represents a warm "end-member" of the sea-ice covers of Antarctica. An expected consequence of the lengthy flooding condition at the snow/ice interface is an earlier onset of an algal bloom in the flooded snow than elsewhere in Antarctic sea ice.

*Corresponding author. Tel.: +603 646 4255; fax: +603 646 4644.
E-mail address: perovich@crrel.usace.army.mil (D.K. Perovich).

0967-0645/$ - see front matter
doi:10.1016/j.dsr2.2004.07.024

1. Introduction

The snow and sea-ice cover of the Antarctic marine ecosystem is a dynamic and important component that is sensitive to interactions with the atmosphere and ocean. The sea-ice cover provides a complex habitat for marine microalgae (Ackley et al., 1979; Palmisano and Sullivan, 1983; Eicken, 1992; Horner et al., 1992; Legendre et al., 1992), krill (Siegel and Loeb, 1995; Quetin et al., 1996), and higher organisms (Ainley and DeMaster, 1990; Trivelpiece and Fraser, 1996). Interactions of different trophic levels with sea ice have been hypothesized and outlined (Ackley and Sullivan, 1994; Smith et al., 1995). Of particular concern to the US Southern Ocean GLOBEC (SO-GLOBEC) program are potential relationships between krill survival and the sea-ice cover (Quetin and Ross, 1991; Quetin et al., 1994; Siegel and Loeb, 1995). The morphology of the sea-ice cover is an important element of the physical environment that strongly influences both the distribution of and the amount of resources available to Antarctic krill (Marschall, 1988; Daly, 1998). The presence of a sea-ice cover also strongly affects the transfer of heat, salt, and momentum between the atmosphere and ocean.

The spatial distribution and temporal evolution of snow depth, ice thickness, and freeboard are complex. Ice deformation results in great variability in ice thickness. Heavy snows can result in flooding of the ice surface with the eventual formation of snow–ice. Studies have indicated that, because of ample snowfall and large ocean heat fluxes, Antarctic sea ice can be melting on the bottom, while it is growing on the surface through snow–ice formation (Lytle and Ackley, 2001). The permeability of the sea ice strongly influences the exchange of salt and nutrients between the ice and upper ocean. Above the critical percolation threshold of 5% brine volume, the ice becomes permeable to rapid fluid transport (Golden et al., 1998; Golden, 2001). The morphology of the ice cover also affects the light regime in and under the ice, which in turn influences the snow algae, ice algae, and water column productivity, as well as the visibility for both predator and prey.

There have been numerous previous studies of physical and morphological properties of Antarctic sea ice and snow (Jeffries et al., 1998; Massom et al., 1997; Sturm et al., 1998; Worby et al., 1998). Granular ice has long been recognized as an abundant structural component of sea ice in the Western Weddell Sea found in amounts roughly equal to or greater than columnar congelation ice (Gow et al., 1982, 1987; Lange, 1988; Lange et al., 1989; Eicken and Lange, 1989; Lange and Eicken, 1991; Ackley et al., 1992; Gow et al., 1992; Lytle and Ackley, 1992). Formation of very significant amounts of granular ice also has been observed in the sea ice of the Western Ross Sea by Jeffries and Weeks (1993); in the eastern Ross, Amundsen, and Bellingshausen Seas by Jeffries et al. (1994); and in the Indian Ocean sector by Allison and Qian (1985), Jacka et al. (1987), and Tison and Haren (1989). Worby et al. (1998) summarized results from several cruises in the East Antarctic region, while Jeffries et al. (1998) reported findings from the Bellingshausen Sea, Amundsen Sea, and Ross Sea. Generally speaking, Antarctic studies have shown a preponderance of deformed first-year ice, considerable surface flooding, large ice salinities, predominantly granular crystal structure, and significant amounts of snow–ice formation.

The Marguerite Bay region was the focus of US Southern Ocean GLOBEC field studies in August and September of 2001 and 2002. Prior to the experiment little was known about the ice properties in this region. Our work was directed at remedying this lack and answering three science questions: (1) what are the basic morphological properties of the ice cover; (2) what are the ice production mechanisms; and (3) was the ice above the percolation threshold? Answering these questions is of importance not only to SO-GLOBEC research, but also to other issues such as the exchange of heat and salt between the atmosphere and ocean and the mass balance of the ice.

2. Instruments and methods

The three science questions were addressed through observations made during the 2001 and 2002 winter cruises of the R.V. *Laurence M. Gould.*

Observations were conducted from the bridge while the ship was en route, surveys of snow and ice thickness and properties were performed from the surface, and measurements were made using autonomous mass balance buoys. The morphological properties of the ice cover were investigated by measurements of the distribution of snow depth, ice thickness, and flooded ice. Observations of the crystallographic structure of the ice were used to gain insight about ice production. Autonomous buoys investigated ice production by monitoring the accretion and ablation at the surface and bottom of the ice. Measurements of ice temperature and salinity were used to compute the brine volume to determine whether the ice was above the percolation threshold.

When the ship was underway, hourly ice observations were made from the bridge using the ASPECT protocol (Worby, 1999). The ice concentration, thickness, ice type, and snow type were recorded for the primary, secondary, and tertiary ice types. These observations provided an estimate of the ice thickness and concentration over the large area of the ship cruise tracks (Fig. 1).

When the ship was stopped it was possible to conduct surface-based surveys of snow and ice morphology. This was done on 10 floes in 2001 and eight floes in 2002. The locations of these measurements sites are shown in Fig. 1 and the dates are listed in Table 1. The 2002 cruise was slightly later, with sites visited between 5 August and 5 September, compared to 28 July–23 August in 2001. Time on station ranged from 1 to 6 days and the level of detail of the measurements varied accordingly. The central element of the snow and ice morphology characterization was surveys of snow depth and ice thickness. Survey lines were selected to include a representative sample of ice conditions. We attempted to make the lines at least 50 m long, but often the floes were small and consequently line lengths ranged from 12 to 126 m. Measurements were made at a 1-m horizontal spacing along these survey lines. First snow depth and flooded layer depth were measured along the entire line. After these measurements were completed, holes were drilled using a 5-cm-diameter auger and ice thickness was measured along the line. Measurements were made using tapes and rulers and had an accuracy of ± 0.5 cm. Twelve survey lines were measured in 2001 and 15 in 2002. In some cases there was sufficient time on station that made it possible to repeat the survey lines to examine ice production and evolution over a 3- to 6-day period.

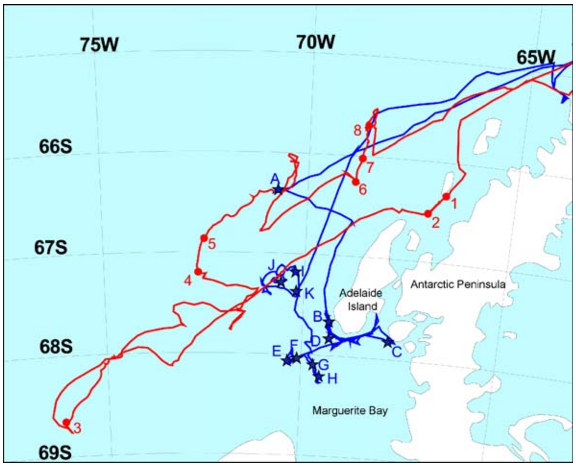

Fig. 1. Map showing cruise tracks and ice study sites of 2001 (blue) and 2002 (red) of the R.V. *Laurence M. Gould*.

Several sites were selected along the survey lines for a more detailed analysis of the snow and ice cover. The presence of ice layers or slush in the snow cover was noted. Typically, four ice cores were taken at each site: one to measure vertical profiles of temperature, salinity, and oxygen isotopes; one to examine the crystal texture and stratigraphy of the ice; and two for biological analysis. The cores were drilled by hand using a 7.25-cm core barrel to avoid contamination by oil and gasoline. Small holes were drilled in the ice properties core at 5- to 10-cm intervals immediately after the core was removed. Ice temperatures were then measured in these holes using a digital thermometer with an accuracy of $\pm 0.1\,^{\circ}$C. One core was sliced into 5- to 10-cm sections, which were placed into separate containers, returned to the ship, and melted. After melting, the salinity was measured using a YSI Model 30 salinometer with an accuracy of 0.1 psu. Measured temperature and salinities were used to compute the brine volume using the relationship of Frankenstein and Garner (1967). Thin sections were made parallel to

Table 1
Summary of thickness survey results

Ice station	Floe ID	Date	Length	Snow				Ice						Freeboard				% Below sea level
				Mean	Std. Dev.	Min	Max	Mean	Std. dev.	Coef. var.	Floe type	Min	Max	Mean	Std. Dev.	Min	Max	
2001																		
Site 1, Floe 1	A	28 Jul	12	18.6	3.7	13	26	65.3	19.3	0.30	Y	49	103	0.1	1.3	−2	3	31
Site 1, Floe 2	A	28 Jul	25	5.7	0.5	5	7	32	0.4	0.01	X	31	33	0.8	0.4	0	2	0
Arched Ice Berg	B	30 Jul	69	15.3	12.1	1	47	60.3	44.6	0.74	Z	17	214	−1.3	7.6	−17	22	37
Leopard Seal	C	1 Aug	10	10.8	5.6	3	19	51.3	22.3	0.43	X	29	95	2.9	7	−6	15	45
Flooding return	D	2 Aug	24	14.4	8.6	4	36	33	9.9	0.30	Y	10	54	−0.3	3	−8	5	48
Robert	E	5 Aug	126	22.7	9.6	4	57	71.4	50.3	0.70	Z	19	235	−2.6	10.6	−17	36	67
Robert	E	9 Aug	32	16.1	5.4	8	32	57.5	19.7	0.34	Y	43	142	0.5	1.5	−3	3	21
Fernando	F	11 Aug	35	23.3	7.5	7	33	43	8.2	0.19	X	33	74	−10.2	7.4	−20	17	89
Backbend	H	12 Aug	15	20.5	11.5	7	38	50.8	16.6	0.33	Y	33	97	−4.8	7.8	−16	15	69
Billy	I	15 Aug	76	6.4	3.9	1	22	75	57.1	0.76	Z	23	280	5.9	10.5	−1	80	1
Billy	I	19 Aug	44	12.8	7	2	31	62.1	46.2	0.74	Z	27	179	3	6.2	−1	32	7
Yoga	J	23 Aug	20	18.3	5.5	8	29	76.8	21.2	0.28	Y	41	119	−1.5	4.8	−8	12	57
All 2001 sites		7/28–8/23	488	16	11	1	57	62	44	0.71		10	280	−0.9	9.5	−20	80	40
2002																		
Levy	1	5 Aug	25	22	2.9	17	27	61.1	7.9	0.13	X	43	75	0.6	2	−3	5	23
Bergie Bit	2	5 Aug	35	44	15.7	21	89	189	85.8	0.45	Z	55	323	9.4	16.7	−14	63	14
Sparky	3	11 Aug	64	10.7	5.6	0	31	79.2	65.4	0.83	Z	22	320	4.9	9.7	−19	40	23
Sparky	3	11 Aug	30	19.5	12.1	7	58	173.2	116.3	0.67	Z	27	388	7.4	19.3	−28	52	26
Sparky	3	17 Aug	9	5	1.4	3	8	34.4	2.7	0.08	X	29	38	1.8	1.5	0	4	0
Minke	4	20 Aug	40	15	9.3	4	45	191.8	56.7	0.30	Y	38	295	14.2	8.6	0	40	0
Minke	4	20 Aug	30	10.8	3	3	19	74.1	30.1	0.41	Z	31	191	3.2	4.2	0	24	0
Rodin	5	22 Aug	100	10.4	7.7	1	41	56.1	39.9	0.71	Z	21	202	3.6	5..9	0	52	0
Rodin	5	22 Aug	30	8.7	4.2	4	17	85.4	68.4	0.80	Z	32	221	5.7	4.8	1	18	0
Rodin	5	25 Aug	60	7.7	5.4	2	27	39.3	8.3	0.21	Y	31	65	2.8	1.3	0	5	0
Rodin	5	28 Aug	50	7	1.2	5	10	38.5	3.1	0.08	X	32	48	2.2	1.1	0	5	0
Free Floater	6	1 Sep	20	32.2	13.3	15	55	50	15.1	0.30	Y	22	87	−9.5	1.5	−12	−6	100
Neptune	7	2 Sep	21	28.2	14.5	15	66	127.7	44.2	0.35	Y	57	185	1.1	8.1	−4	34	55
Deep Dish	8	5 Sep	25	72.9	7.9	50	83	213.8	64.7	0.30	Y	83	333	0.9	9.4	−7	37	73
Deep Dish	8	5 Sep	25	90.3	26.4	37	140	305.9	120.7	0.39	Y	160	565	13.4	32.5	−4	110	40
All 2002 sites[a]		8/5–9/5	564	20.9	23.6	0	140	102.1	92.1	0.90		21	565	4.5	11.5	−28	134	17

All thicknesses and depths are in cm. Floe type refers to the classification system of Jeffries et al. (1998).

[a]except for Deep Dish.

the vertical axis of the structure cores. These thin sections were photographed in both transmitted natural light and between crossed polarizers to determine the ice type and crystallographic structure. Samples from the snow and the ice sections also were used for a post-experiment oxygen isotope analysis. Delta ^{18}O determinations used the traditional method of CO_2 equilibration with water (Epstein and Mayeda, 1953). After one day of equilibration at 25 °C, the CO_2 was analyzed with a dual inlet triple ion collection (masses 44, 45, and 46) mass spectrometer built with Micromass components. Laboratory working standards calibrated using IAEA reference waters were measured with the samples daily. Isotope data are reported using the conventional delta notation in terms of the standard V-SMOW (Coplen, 1996). The standard deviation of the measurements was ±0.2‰.

In addition to the surveys, we installed two custom-made CRREL ice mass balance buoys in 2001 and two in 2002 (Perovich and Elder, 2001; Morison et al., 2002). These buoys provided a means to obtain temporal information on ice production and on percolation in the ice. Fig. 2 presents a schematic of a mass balance buoy plus a photograph of an installed buoy. The buoys had a thermistor string that measured a vertical profile of temperature, at 5-cm spacing, from the air, through the snow and ice, and into the upper ocean. There were acoustic sensors measuring the positions of the snow surface and ice bottom. Barometric pressure, position, and air temperature also were measured. All buoy data were transmitted via Service ARGOS. The combination of thin ice, high winds, and considerable ice deformation made this a harsh environment for these mass balance buoys. However, in each year one mass balance buoy survived for more than 3 months, providing a temporal record of the ice evolution.

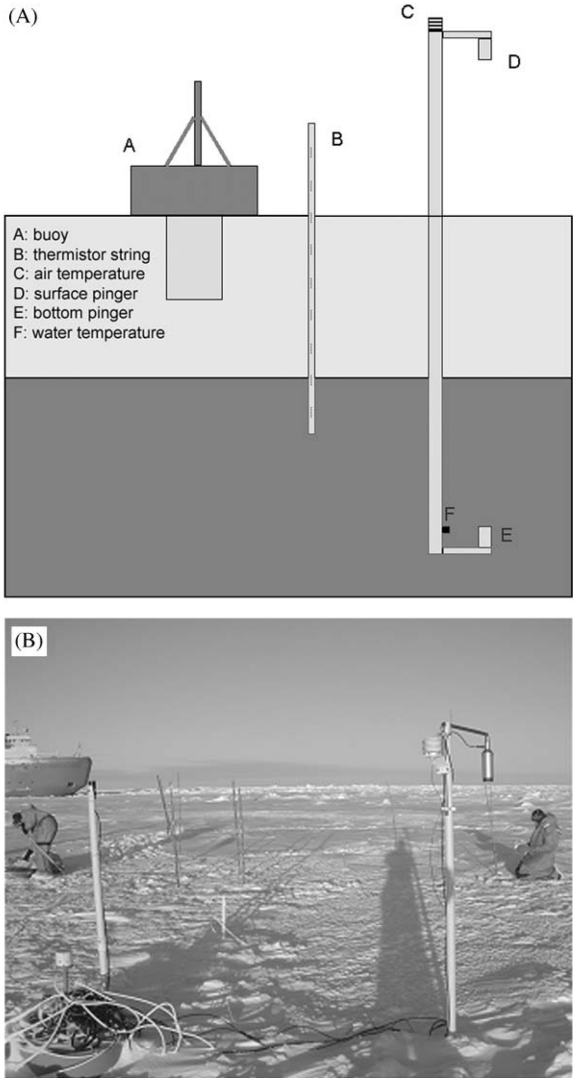

Fig. 2. The autonomous mass balance buoy: (A) buoy schematic and (B) photograph of an installed buoy.

3. Results

3.1. The morphological properties of the ice cover

The basic morphological properties of the ice cover include the ice extent, ice thickness, snow depth, and freeboard. The overall development of the ice cover was markedly different in 2001 and 2002. (Fig. 3). There was more ice present in 2002 throughout the entire fall–winter period in the Western Antarctic Peninsula region. During 2002 there was ice present in Marguerite Bay even in March, and there was ample ice coverage in the entire region by late June. In contrast, in 2001, the Western Antarctic Peninsula region into Marguerite Bay was open until late June. These differences

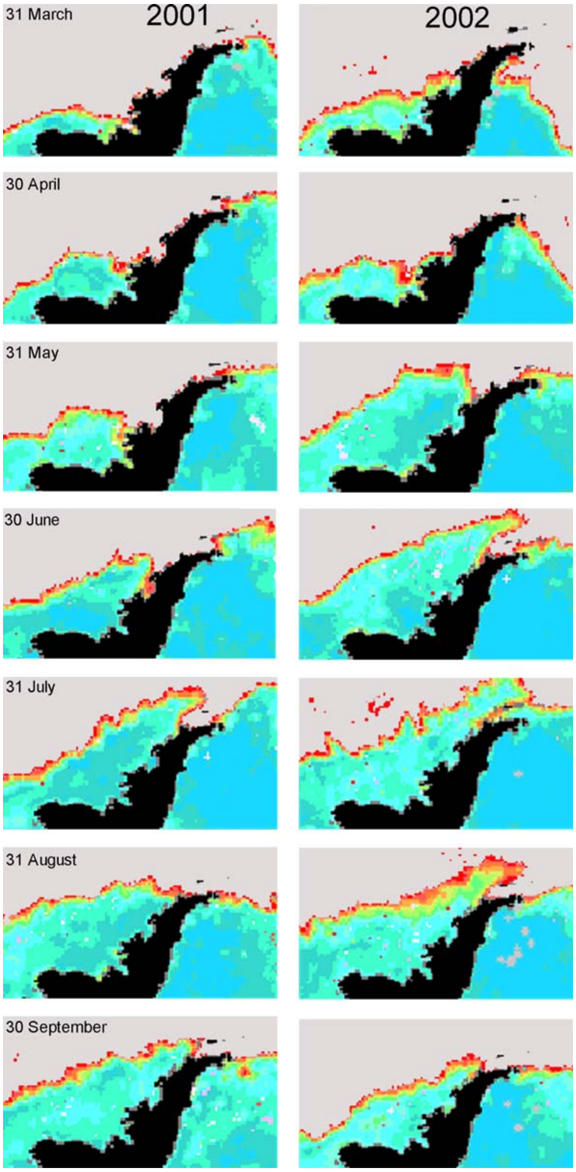

Fig. 3. Regional ice extent and concentration as a function of time for 2001 and 2002 as derived from Special Sensor Microwave Imager (SSM/I) satellite data (NOAA Web site).

are consistent with our experience cruising in the pack in 2001 and 2002. In 2001 with the ice edge closer to mainland Antarctica, south of Palmer Station, we were able to maneuver in the coastal leads and polynas into the northern reaches of Marguerite Bay with little difficulty. In contrast, during 2002 we encountered the ice edge north of Palmer Station and the Antarctic Peninsula, making passage more difficult. The larger extent of the ice created more forcing on the ice from the winds, creating higher amounts of ridged ice and an ice pack that was frequently under pressure, preventing us from even entering Marguerite Bay. Therefore, our 2002 studies were farther offshore than in 2001, but still well within the ice pack.

Each year hourly ice observations were made while the ship was underway in the ice. The average ice thickness derived from these measurements, not including areas of open water, was 46 cm in 2001 and 56 cm in 2002. The distribution of ice thickness, grouped into 10-cm bins, is presented in Fig. 4. Although in both years the peak of the ice thickness distribution was the 40- to 50-cm bin, there were distinct differences. In 2001 there was more ice thinner than 40 cm and less ice thicker than 60 cm.

When the ship was stopped, it was possible to get on the ice and make detailed surveys of the snow depth, freeboard, and ice thickness. During the two field campaigns, we measured a total of 27 thickness survey lines; 12 in 2001 and 15 in 2002, for a total of 1052 points. Table 1 summarizes the results from individual surveys and cumulative averages for each year. In 2002, there was a search for an extremely thick floe. This floe, "Deep Dish," was not representative of the general ice pack, and results from the surveys on it are not included in the summary statistics. Results from

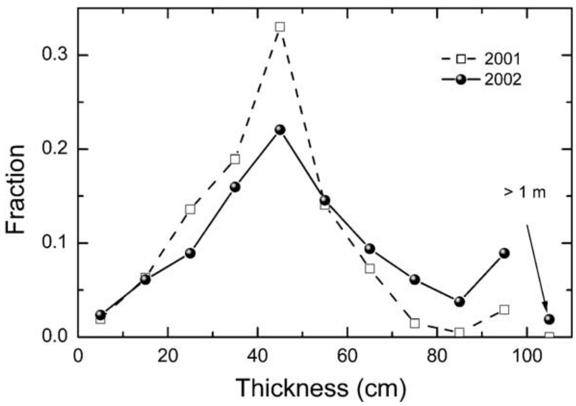

Fig. 4. Probability distributions of ice thickness grouped into 10-cm bins in 2001 and 2002 determined from bridge observations made while the ship was en route in the ice.

individual measurements were combined to calculate probability distributions of ice thickness, snow depth, and freeboard (Fig. 5). Data were grouped using 5-cm bins for snow depth and ice thickness and 1-cm bins for freeboard. Though 2 years do not make a climatology, the comparisons between 2001 and 2002 provide a limited, but still useful, perspective on the interannual variability of ice conditions in the Marguerite Bay region.

The ice was much thicker in 2002, with an average value of 102 cm compared to 62 cm in 2001. This is consistent with the earlier ice formation in 2002 and with the fact that the 2002 measurements were made later in the growth season. The 2001 ice thickness distribution has a sharp peak at 30–35-cm, with over half of the thicknesses between 30 and 50 cm (Fig. 5B). The 2002 peak was also 30–35 cm, but it was much less pronounced than in 2001 and only 27% of the thicknesses were between 30 and 50 cm. There was more thick ice (>1 m) in 2002, implying greater deformation that year.

A key difference between the 2 years was in the average freeboard: -1 cm in 2001, compared to 5 cm in 2002. The freeboard probability distribution is centered around 0–1 cm, tapering off towards negative and positive values. In 2001, the negative portion of the distribution is larger than the positive, while in 2002 the opposite is true. Indeed, 52% of the ice had a freeboard $\leqslant 0$ in 2001, compared to only 20% in 2002, implying a greater opportunity for surface flooding and snow–ice formation in 2001.

The average snow depth was 21 cm in 2002 compared to 16 cm in 2001. In both years the snow depth distribution had a broad peak in the 5- to 30-cm range. There was more deep snow in 2002, with 11% of the snow depths being greater than 50 cm, compared to less than 1% in 2001. However, it should be noted that in 2001 over half the ice had negative freeboard and considerable surface flooding was observed. It is possible that this flooding and the subsequent formation of snow–ice, reduced the depth of the snow cover in 2001 (Jeffries et al., 2001).

The roughness of the ice is an important consideration for the redistribution of windblown snow, for ice production, and for the underice

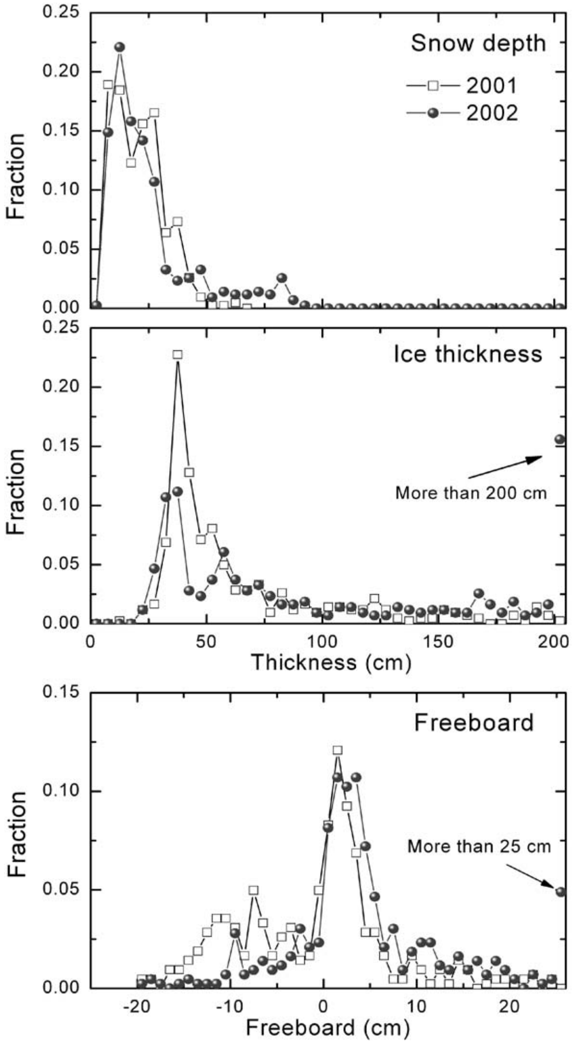

Fig. 5. Probability distributions of (A) snow depth, (B) ice thickness, and (C) freeboard for 2001 and 2002 determined from survey profiles.

habitat. Jeffries et al. (1998) classified floes into three basic categories based on ice roughness and ridging. The categories were defined using the ratio of the standard deviation (σ_i) and mean ice thickness (μ_i) and corresponded to σ_i /μ_i ranges of 0–0.19 (X), 0.2–0.39 (Y), and above 0.4 (Z). Applying this criterion to our data (Table 1), there were 6 X areas (22%), 11 Y areas (41%), and 10 Z areas (37%). Compared to the Jeffries et al. (1998) results from the Amundsen and Ross Seas, the Marguerite Bay region had fewer smooth areas (X) and more rough areas (Y, Z). We believe that the greater spatial variability in ice thicknesses in Marguerite Bay was a result of an ice pack that was more broken up, with smaller floes, and more deformed ice.

Detailed transect data are presented in Fig. 6 for ice floes representing these three types. Floe A was one of only a few X-type floes we encountered, where the ice appeared smooth and there were no signs of deformation (Fig. 6A). The snow depth was 5–8 cm and the entire transect had positive freeboard. Fig. 6B presents a profile of a Y-type floe, the unusually thick, 2002 cruise ''Deep Dish'' floe. This was the thickest floe sampled, with an average thickness of 305 cm and a range from 150 to 450 cm. This floe also had the deepest snow, averaging 90 cm and ranging from 37 to 140 cm. As the snow profile in Fig. 6B indicates, the large pressure ridge acted as a collector, building a snowdrift. This was not surprising as high winds and blowing snow were frequently observed during the experiment. Because of this deep snow, even though this was the thickest ice measured, 40% of the transect line was below sea level and flooded. Typical of the most common floes encountered was the Z-type floe measured on Floe E (Fig. 6C). The 50-cm-thick ice has undergone considerable ridging, forming several 1- to 2-meter keels and 0.2- to 0.5-m sails that were effective in collecting snow. This floe had the deepest snow of the 2001 field experiment. This resulted in a 10-cm-thick flooded layer that covered two-thirds of the transect line.

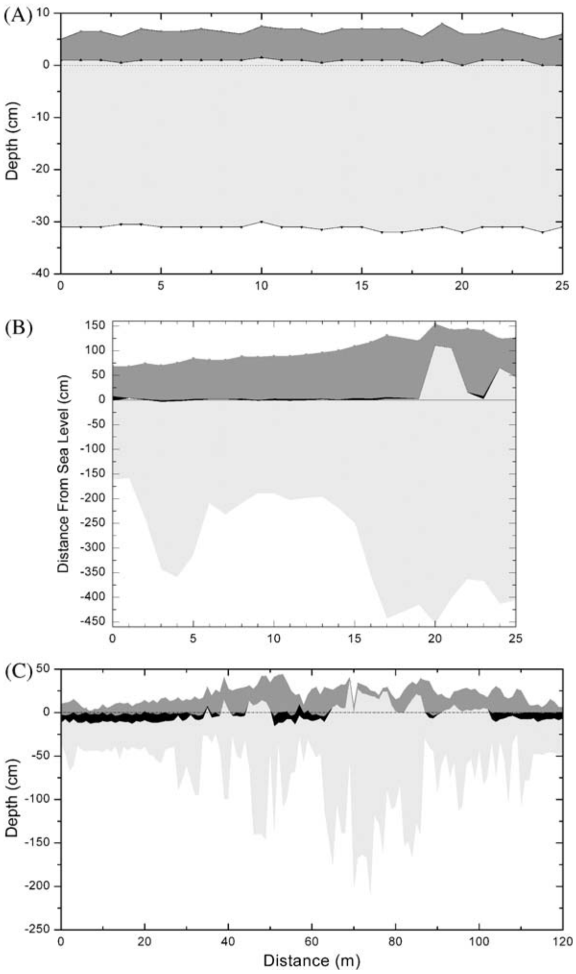

Fig. 6. Selected profiles from ice thickness surveys illustrating (A) undeformed ice (type X), (B) thick ice (type Y), and (C) highly deformed ice (type Z). Dark gray is snow, light gray is ice, black is flooded ice and snow, and white is the air (above) and the ocean (below).

3.2. Ice production

The ship- and surface-based surveys provide a broad picture of the ice cover—its thickness and snow depth, and whether there is flooding. However, by nature, these surveys were snapshots in time, and did not provide information on the formation and evolution of the ice cover. The crystallography of the ice provides a window into its origin and formation. There were 31 such windows in 2001 and 20 in 2002, where an ice core was removed for detailed crystallographic analysis.

The ice core analysis included vertical thin sections photographed under natural and polarized light plus profiles of temperature, salinity, brine volume, and $\delta^{18}O$. The two major components of sea ice are granular ice and columnar congelation ice. Congelation ice is formed by direct freezing of seawater to the underside of an existing ice sheet under quiescent conditions. Granular ice includes frazil ice and snow–ice. Frazil ice forms under turbulent conditions when there is wind- or wave-driven mixing. Frazil ice production is usually more rapid than columnar congelation growth. Snow–ice formation occurs when snow is infiltrated by water that freezes. It is not possible to distinguish accurately between frazil ice and snow–ice by visual inspection under either natural or polarized light. However, the two granular ice components can be readily identified by their differing stable isotopic composition. $\delta^{18}O$ values trend towards more negative values in snow–ice relative to frazil ice, which generally possesses slightly positive values. Following the established protocol (Jeffries et al., 2001), negative $\delta^{18}O$ values were assumed to be snow–ice and positives values frazil ice. The snow–ice fraction was estimated from ice core samples that were melted and returned to the laboratory for $\delta^{18}O$ analysis.

Results from three examples representing cores with small, moderate, and large amounts of granular ice are presented in Fig. 7. The first core had a large amount of columnar ice and was indicative of ice grown under quiescent conditions (Fig. 7A). At this site the ice was 31 cm thick and the snow was 7 cm deep. The top 7 cm of the ice was coarse-grained granular ice and the remainder was columnar. All of the $\delta^{18}O$ samples were >0‰, indicating that no snow–ice was present and that the granular ice was frazil. This core was unusual in its relative lack of granular ice (23%). The second example (Fig. 7B) was similar in crystal structure to the first from a depth of 10 cm to the bottom. The difference was in the top 10 cm, where the fine-grained granular ice and the $\delta^{18}O$ values of -2 to -8‰ indicate that it was snow–ice. Indeed, snow–ice formation was continuing at this site during the measurements. The ice freeboard was negative and the bottom 8 cm of the snowpack was wet and slushy. Fig. 7C shows results from 48-cm-thick ice that consisted entirely of granular ice, aside from the bottom few centimeters that were columnar ice. This ice was warm (-2 to $-3\,^{\circ}C$) and nearly isothermal. Brine volumes were quite large, 20–24% near the surface and 10% at depth. Once again the freeboard was negative and the bottom of the snowpack was wet and slushy. The $\delta^{18}O$ values indicate that the top 22 cm were snow–ice and the remainder of the granular ice was frazil.

Ice core results are summarized in Table 2. Analyzing all the cores indicated that there was a

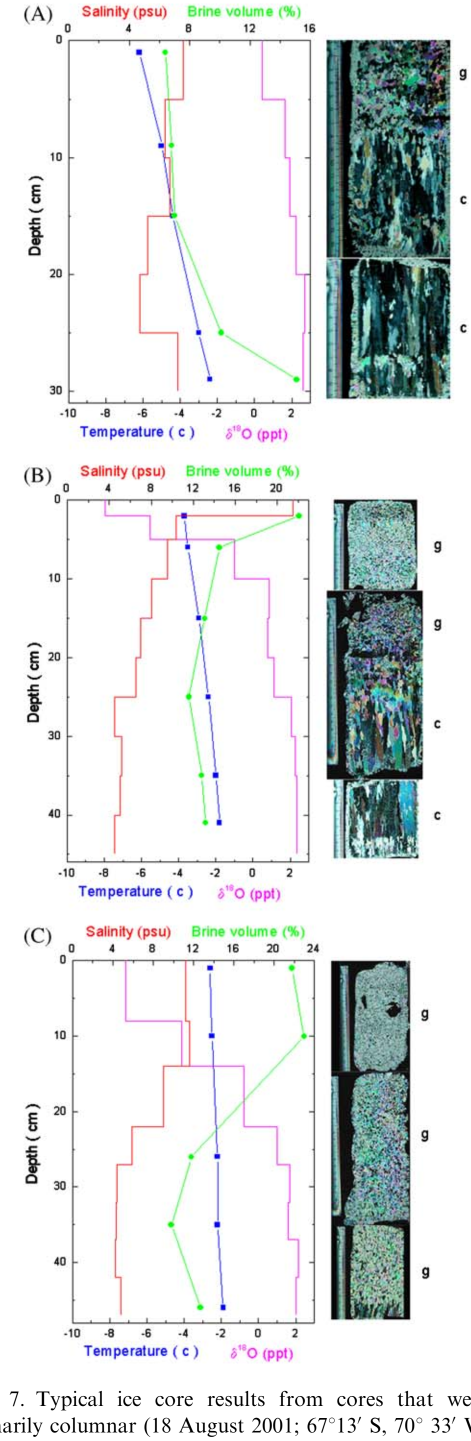

Fig. 7. Typical ice core results from cores that were (A) primarily columnar (18 August 2001; 67°13′ S, 70° 33′ W), (B) granular and columnar with a surface layer of snow–ice (9 August 2001; 68° 02′ S, 70° 07′ W), and (C) snow–ice and granular (12 August 2001; 68° 12′ S, 69° 31′ W).

Table 2
Summary of ice physical properties cores

Date	Latitude (S)	Longitude (W)	Length	H_i	F_b	S_b	Granular (%)	Columnar (%)	Snow–ice (%)
7/28/2001	66 21.3′	70 43.1′	50			5.4	40	60	0
7/28/2001	67 21.6′	71 43.1′	33			5.8	53	47	0
7/30/2001	68 39.5′	70 20.0′	33	32	1	8.9	40	60	15
7/30/2001	67 39.8′	69 20.4′	45	40	1	6.2	73	27	33
8/1/2001	67 49.2′	67 48.0′	30	31	1	6.7	68	32	30
8/2/2001	67 49.5′	69 18.8′	35	34	2	7.5	37	63	31
8/6/2001	68 04.1′	70 11.2′	86	86	7.5	7.7	25	75	0
8/6/2001	68 04.2′	70 11.9′	32	29	−7	6.7	59	41	
8/6/2001	68 04.4′	70 13.2′	167	183	14	6.6	76	24	0
8/7/2001	68 01.2′	70 20.2′	40	39	−8	7.0	58	42	10
8/7/2001	68 01.2′	70 20.2′	52			6.8	80	20	0
8/7/2001	68 01.2′	70 20.2′	47	47	13	4.6	100	0	0
8/7/2001	68 01.2′	70 20.2′	28	33	3	6.3	100	0	53
8/7/2001	68 01.2′	70 20.2′	147	165	12	7.4	48	52	7
8/7/2001	68 01.2′	70 20.2′	52	51	4	8.2	54	46	49
8/7/2001	68 01.2′	70 20.2′	44	47	3	7.4	43	57	35
8/9/2001	68 02.1′	70 06.8′	42	42	0		43	57	13
8/9/2001	68 02.1′	70 06.8′	44	44	0	7.4			27
8/11/2001	68 05.5′	69 41.5′	54	52	1	8.8	28	72	24
8/11/2001	68 05.5′	69 41.5′	44				40	60	
8/12/2001	68 12.3′	69 31.1′	50	49	2	7.4	95	5	47
8/16/2001	67 08.5′	70 14.6′	24	25	0	6.7	69	31	14
8/16/2001	67 08.5′	70 14.6′	36	40	−3	5.6	84	16	0
8/16/2001	67 08.5′	70 14.6′	30	33	3	7.8	19	81	13
8/16/2001	67 08.5′	70 14.6′	46			7.2	100	0	41
8/16/2001	67 08.5′	70 14.6′	115	142	5	8.7	86	14	22
8/16/2001	67 08.5′	70 14.6′	49		3	7.3	97	3	0
8/18/2001	67 12.9′	70 33.0′	30	30	0	6.3	65	35	0
8/19/2001	67 17.1′	70 35.1′	34	35	0	8.7			41
8/16/2001	67 08.5′	70 14.6′	31	32	0	5.9	66	34	16
8/20/2001	67 11.3′	70 49.2′	64	64	20	6.1	47	53	0
8/21/2001	67 24.8′	70 49.6′	164	164	−3	5.5	84	16	6
8/23/2001	67 22.3′	70 11.8′	76		3	7.4			10
8/5/2002	66 20.4′	66 40.8′	58	59	0	6.2	92	8	
8/6/2002	66 31.2′	67 04.8′	108	119	1	6.9	62	38	
8/11/2002	68 40.2′	76 10.8′	31			7.9	100	0	
8/11/2002	68 40.2′	76 10.8′	180	179	19	5.5	92	8	
8/14/2002	68 10.2′	75 11.4′	177			7.1	73	27	
8/15/2002	68 05.4′	75 01.2′	70	72	1	8.6	92	8	
8/16/2002	68 01.8′	74 51.0′	34	31	1	7.3	100	0	
8/19/2002	67 30.0′	71 30.0′	117	141	25	6.4	86	14	
8/21/2002	68 05.4′	72 39.6′	31			6.0	88	12	
8/21/2002	68 05.4′	72 39.6′	166	206	15	6.9	47	53	
8/23/2002	66 42.6′	72 10.2′	221	255	7	8.8	—	—	
8/24/2002	66 38.4′	71 58.8′	300			7.9	100	0	
8/26/2002	66 23.4′	71 09.6′	72	66	0	6.5	37	63	
9/1/2002	66 15.6′	68 52.2′	63	60	−6	6.8	35	65	
9/2/2002	66 01.8′	68 44.4′	64	64	−3	6.8	75	25	
9/2/2002	66 01.2′	68 44.4′	152	173	6	7.1	78	22	
9/4/2002	65 46.2′	68 40.2′	75	72	−6	8.6	100	0	
9/6/2002	65 42.6′	68 43.2′	60	67	2	11.5	86	14	
9/7/2002	65 37.2′	68 36.0′	87	88	5	5.9	—	—	
9/7/2002	65 37.2′	68 36.0′	83	80	2	5.8	95	5	
9/8/2002	65 31.2′	68 29.4′	44	79	2	7.6	79	21	

Length is the core length (cm), H_i theice thickness (cm), F_b the freeboard (cm), and S_b the bulk salinity (psu).

preponderance of granular ice, consistent with the findings of earlier studies (Gow et al., 1987; Lange, 1988; Eicken and Lange, 1989; Lange and Eicken, 1991; Jeffries and Weeks, 1993; Jeffries et al., 1994; Worby et al., 1998). There was more granular ice in 2002 (78%) than in 2001 (66%). Overall the granular fraction of individual cores ranged from 20% to 100%. In 2002, 85% of the cores were more than half granular ice compared to 65% of the cores in 2001. Many of the cores, 20% in 2002 and 10% in 2001, were composed entirely of granular ice. The abundance of granular ice confirms our qualitative observation that growth conditions in the study area typically were turbulent, favoring frazil production over congelation growth. Also, a significant portion of the ice surface was flooded, leading to snow–ice formation.

The frequency distribution of $\delta^{18}O$ values for the samples taken in 2001 is plotted in Fig. 8A. Most of the samples (85%) had positive $\delta^{18}O$ values, though 15% had negative values, implying that it was snow–ice. Examining the $\delta^{18}O$ results on a core-by-core basis indicated that 32% of the cores had no snow–ice, 23% had a small amount in the top few centimeters of ice, and 45% were at least 15% snow–ice. Fig. 8B displays all the measured $\delta^{18}O$ values for 2001 as a function of depth within the ice. Most of the negative $\delta^{18}O$ values were from the top 10 cm of the ice and virtually all were from the top 20 cm. The one exception was a negative value found at a depth of 50 cm. This was in a core that showed strong evidence of ice deformation and a likelihood that the 50-cm-deep sample was once at the surface.

At a few sites, we were able to obtain a brief glimpse of the temporal evolution of the ice cover by repeating the thickness survey along the same transect a few days later. Fig. 9A shows results from a 30-m transect made on 5 August 2001 and repeated on 9 August 2001. Initially, the entire transect was below freeboard and the surface was flooded with a 5- to 10-cm slush layer. After 5 days of air temperatures between $-10\,^{\circ}C$ and $-4\,^{\circ}C$, this slush layer froze, forming snow–ice (Fig. 9B). However, there was essentially no bottom growth of the ice cover during this period. The heat lost from the ice cover to the atmosphere resulted in freezing of the slush layer, not bottom growth. There was evidence of modest deformation around 15 m and significant ridging at 28–30 m, illustrating the important of ice dynamics in this region. In 2002, repeat measurements were made at a 30–40-cm-thick floe that had a thin 5–10-cm snow cover. On 22 August 2002 the freeboard was positive along the entire transect and there was no surface flooding (Fig. 9C). Six days later on 28 August 2002, the repeat of the transect (Fig. 9D) showed an accumulation of a few centimeters of new snow bottom ice growth of 3–5 cm everywhere along the line. Air temperatures ranged from -25 to $-4\,^{\circ}C$, averaging $-13\,^{\circ}C$ during this period. In this case, with no flooded layer to freeze, there was columnar ice growth at the bottom.

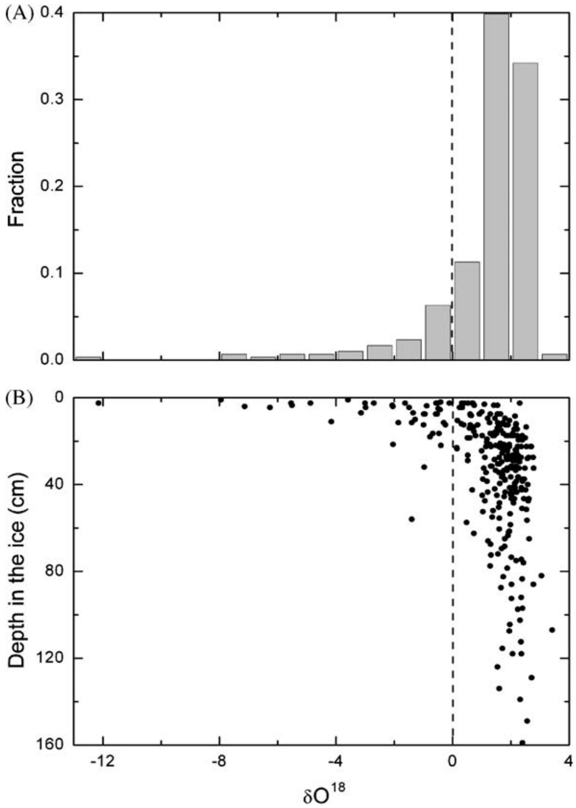

Fig. 8. $\delta^{18}O$ results from samples taken from the 2001 ice cores: (A) probability distribution of $\delta^{18}O$ values and (B) scattergram of $\delta^{18}O$ versus sample depth within the ice.

The autonomous mass balance buoys also provide information on the formation and

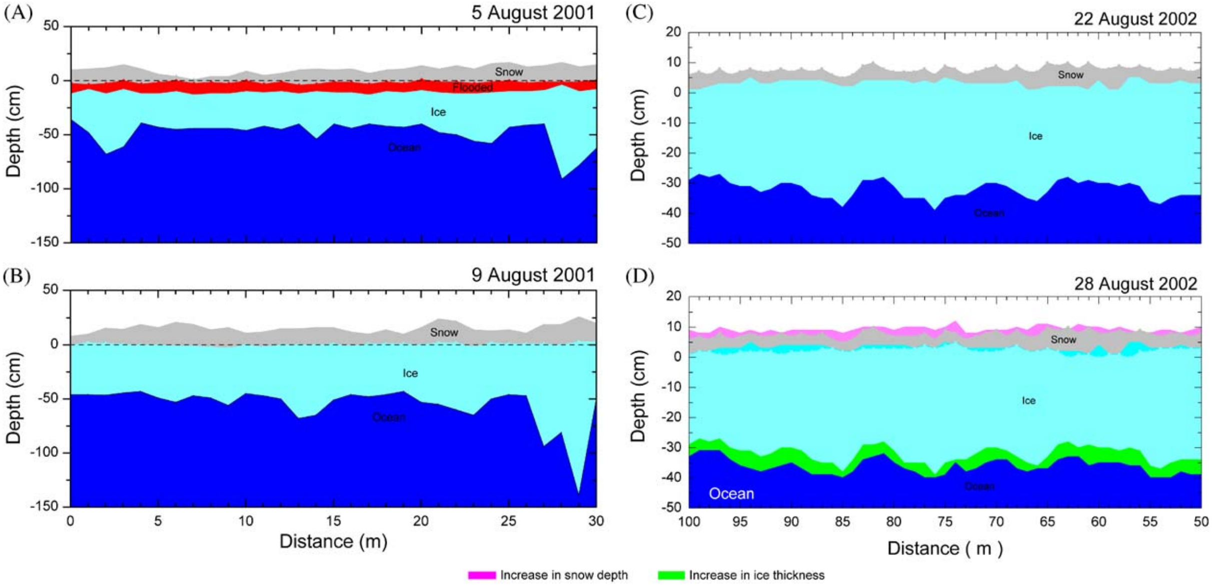

Fig. 9. Before and after repeat thickness surveys in 2001 showing freezing of flooded layer and in 2002 showing bottom growth. The panels are (A) 5 August 2001, (B) 9 August 2001, (C) 22 August 2002, and (D) 28 August 2002.

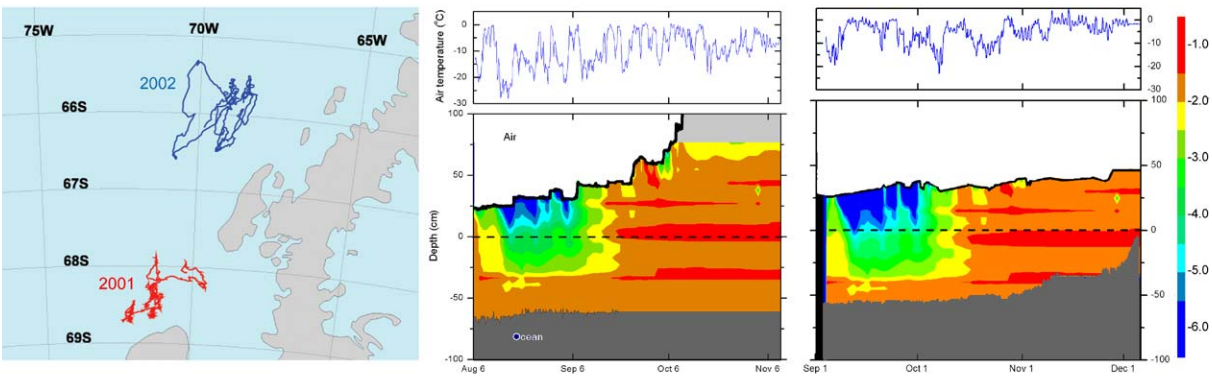

Fig. 10. Time series results from the autonomous mass balance buoys of (A) drift tracks and mass balance from (B) 6 August to 10 November 2001, and (C) 4 September to 5 December 2002. Internal ice temperature is displayed using color contours, with blue being cold (−6 °C) and red warm (0 °C). The black/white interface denotes the changing position of the snow surface, the dashed black line the original position of ice surface, and the bottom boundary between orange and gray the ice/ocean interface. The gray portion in panel (B) is snow where there were not any temperature measurements. The ice bottom sensor in 2001 failed on 20 September and a flat line is plotted after this date.

evolution of the ice. Results from the two longest lasting mass balance buoys in 2001 and 2002 are presented in Fig. 10. The data record for each buoy was approximately 3 months long, with a period of data overlap between 4 September and 10 November for the 2 years. We believe that the 2001 buoy was destroyed during an ice deformation event, while in 2002 the buoy was lost when the ice melted.

The defining feature of the 2001 time series was the heavy snowfall. When the buoy was installed there were 25 cm of snow, 65 cm of ice, and a freeboard of −1 cm. The snow depth increased by more than 1 m between 6 August and 6 November. The temperature record indicates the ice was warm and, given the initial ice salinity of 5–10 psu, the brine volume was large. The temperature record also shows warm intrusions (red bands in Fig. 10B), presumably due to surface flooding. With air temperatures below freezing, this flooding could lead to substantial snow–ice formation. Assuming that (1) as the snow depth increases, the floe sinks to remain in hydrostatic equilibrium; (2) there is brine percolation in the ice; (3) the surface floods as the floe sinks; and (4) if the flooded snow freezes into ice, then there would be 68 cm of snow–ice formation at this site. This would double the initial ice thickness of 67 cm. In contrast, there was only 20 cm of snow accumulation at the buoy in 2002 and no evidence of snow ice formation.

There was little growth (< 5 cm) at the bottom of the ice in either year. The bottom record from 2001 is limited, since the under-ice sensor failed midway through the experiment. However, to this point there had been no bottom ice growth and approximately 5 cm of bottom ablation. In addition, the temperature profiles exhibited very weak thermal gradients limiting ice growth. The 2002 bottom sensor record is complete and shows no bottom growth and two periods of significant bottom ablation. The first was between 1 November and 11 November, when the ice thinned by 13 cm from 49 to 36 cm. The second was the final melting of the floe, which began on 25 November, ending with the demise of the buoy on 2 December 2002. Overall the buoy results indicate that there was little columnar ice growth, but there was considerable slush formation with some snow–ice formation.

Ice production in Marguerite Bay was similar to that found in other Antarctic sea-ice regions. There was a highly variable mix of granular and columnar ice, but overall a preponderance of granular ice. The granular ice was primarily frazil, but snow–ice was significant, comprising from 0% to 41% of individual cores and 15% overall. Ice production was strongly influenced by the snow cover. Deep snow resulted in negative freeboard, surface flooding, and the formation of slush and snow–ice. Surface flooding stopped the growth of columnar ice at bottom of the ice. In some cases there was even bottom ablation, which tended to reduce the relative amount of columnar ice.

3.3. Percolation in the ice

When the brine volume of the ice exceeds a critical threshold of 5%, the sea ice becomes permeable enough that percolation can occur and the transport of brine within the ice matrix is greatly enhanced (Golden et al., 1998; Golden, 2001). This transport is of great importance, as it contributes to the flooding of the ice surface as well as affecting the distribution of nutrients within the ice. The ice core measurements of temperatures and salinities along with the computed brine volumes provide insight on the amount of ice above the percolation threshold. Even though air temperatures were cold during the cruises, the combination of deep snow and thin ice resulted in warm temperatures throughout the ice. As was noted earlier, ice salinities were large, typically ranging from 5 to 9 psu. The brine volumes of the ice sampled were typically above the critical percolation threshold regardless of the ice thickness or crystallography. For example, the ice crystallography of the three cores in Fig. 7 was quite different, but their temperatures, salinities, and consequently brine volumes were similar. The three cores were above the percolation threshold at all depths. Analyzing the brine volume profiles from all the ice cores showed that in 2001 the mean brine volume was 12.9%, with a range from 2.9% to 31.5%. Results from 2002 were roughly comparable, with a mean brine volume of 16% and a range from 1% to 37%. Most important, in 2001, 95% of the ice sampled was above the critical threshold and 97% was above in 2002.

The mass balance buoys were used to extend the percolation data set. When the buoys were installed the ice salinities ranged from 5 to 10 psu. The ice temperatures measured by the buoys were used to calculate the brine volume, with the assumption that the initial ice salinity profile did not change appreciably over time. From August to December, air temperatures typically ranged from −20 to 0 °C, with changes of 15 °C in a day common. Even though air temperatures were as cold as −20 °C, temperatures in the ice were warm in both years, ranging from 0 to −6 °C as a result of the combination of thin ice and deep snow. From mid-September on, ice temperatures were never colder than −2.5 °C. These temperatures translated to brine volumes ranging from 5% to 30%. The brine volumes were above 5% percolation threshold throughout the ice for the entire lifetime of the buoys. The in situ measurements and the results from the autonomous buoys indicate that the vast majority of the ice sampled in the Marguerite Bay region in late winter and early spring was above the percolation threshold, allowing rapid transport of brine, and of nutrients, within the ice matrix.

4. Discussion

Two-thirds of the cores had some snow–ice and 15% of the ice sampled in 2001 was snow–ice, i.e., an average of ~10 cm in a core of ~60-cm length. Although significant, the high incidence of surface flooding at the time of observation (40%) suggests snow–ice formation is potentially higher. This is also seen by the mass balance buoy observations where flooding and warm temperatures coupled with more than 1 m of snow accumulation showed that an additional 67 cm of snow was flooded at that location. As well, we found that for 95% of the ice sampled at other locations, the combination of warm ice temperatures and large salinities resulted in brine volumes that were greater than the percolation threshold of 5%. Time series from the autonomous mass balance buoys confirmed that high temperatures, consistent with percolation and surface flooding, prevailed at the ice surface throughout late winter and spring.

In comparison, the Weddell Sea pack ice has substantially different character for both the older ice in the western Weddell Sea and the first-year ice in the eastern Weddell Sea. In the eastern part, intermittent flooding is observed during winter. Ice surface temperatures cycle between just above and just below percolation in the winter there (Golden et al., 1998). This case leads to cycling of flooding and snow–ice formation on periods of a few days as air temperature rises and falls with the storm cycle. Coupled with this flooding is the melting of ice from the bottom because of upwelled ocean heat flux (McPhee et al., 1996). This coupled cycle of melting from below (keeping the freeboard near zero) and freezing of flooded snow from the top can lead to the whole vertical profile being composed of snow–ice (Lytle and Ackley, 2001), i.e. 100% snow–ice rather than the 15% snow–ice we observed here.

In the western Weddell Sea, a cold extreme is observed. Ice lasting through the summer has flooded surfaces that freeze up quickly in fall. The freezeup institutes convective overturning of seawater in the near-surface ice and the upwelling of nutrients in the seawater triggers a fall algal bloom in the ice near the surface. Once frozen, however, ice surface temperatures there are below the percolation threshold until well into spring (Lytle and Ackley, 1996). Snow–ice formation is therefore limited to the fall freezeup with no percolation in the winter because of low temperatures, followed by flooding in late spring. No additional snow–ice formation takes place then because of the general increase in air temperatures assisted by high incident solar radiation after the equinox. Instead, some melting in the snow leads to the formation of superimposed ice on the top of the flooded seawater layer (Haas et al., 2001).

The Western Antarctic Peninsula sea ice can therefore be considered as the "warm end member" in the spectrum of flooding and snow–ice formation in the Antarctic sea ice zone. The combination of thin ice, enough snow, and cold air temperatures that allow snow–ice formation apparently exists only in the late fall–early winter period, leading to flooding and snow–ice formation accumulating to the 15% of the vertical ice cover observed in our core profiles. In mid-late winter, heavy snowfall continues to depress the surface below sea level (e.g., >1 m at the mass balance buoy site) and leads to substantial flooding, for example, an additional 67-cm-thick flooded layer at the mass balance site. At the same time, however, the slightly warmer air temperatures and increased snow depth keep ice surface temperatures high enough to prevent additional snow ice formation and to also allow continuous flooding (as observed where 95% of the ice cover is above the percolation threshold).

The extended "spring" of the WAP sea ice, in having a substantial flooded layer from early August to December, can lead to higher sustained levels of algal production in the snow–ice community (Ackley and Sullivan, 1994) than observed elsewhere in the Antarctic sea ice. Access to this algal production by juvenile krill also may be better here than elsewhere because of the substantially porous nature of the ice, indicated by its high percentage above the percolation threshold.

5. Conclusions

At the beginning of this paper, three questions were posed concerning the ice morphology, the formation processes of the ice, and percolation in the ice. The sea ice in this region can be considered as the "warm end member" in the spectrum of flooding and snow–ice formation in the Antarctic sea ice zone. In the late fall–early winter period there is a combination of thin ice, enough snow, and cold air temperatures leading to flooding and snow–ice formation, accumulating to the 15% of the vertical ice cover observed in our core profiles. In mid-late winter, heavy snowfall continues to depress the surface below sea level and leads to substantial flooding. However, the slightly warmer air temperatures and increased snow depth keep ice surface temperatures high enough to prevent additional snow–ice formation and to allow continuous flooding (as observed where 95% of the ice cover is above the percolation threshold). There was considerable interannual variability in ice thickness, with average values of 62 cm in 2001 and 102 cm in 2002. The mean snow depth was 16 cm in 2001 and 21 cm in 2002. At 40% of the thickness holes in 2001 and 17% in 2002, a combination of deep snow and thin ice resulted in negative freeboard and surface flooding.

A stratigraphic analysis of ice thin sections showed that more than half of the ice cover was granular and that virtually all of the upper 20 cm of the ice cover was granular. There was little bottom ice accretion observed, even though air temperatures were as cold as $-20\,^{\circ}\mathrm{C}$. There were indications that snow–ice formation at the surface contributed significantly to ice formation. At most sites the base of the snow cover was wet and saline, indicating flooding. A $\delta^{18}O$ analysis of ice cores taken in 2001 indicated that 15% of the samples had negative values, implying that the sample was snow–ice. Between August and November 2001, mass-balance buoy results indicated over 1 m of snowfall, resulting in considerable snow–ice formation.

Ice core observations indicated that, as a result of a combination of warm ice temperatures and large salinities, brine volumes were typically greater than the critical percolation threshold of 5%. Over 95% of the ice sampled was in a percolation regime, creating the potential for rapid transport of brine and nutrients within the ice matrix. Also, results from the mass-balance buoys indicated that the ice sampled was always above the percolation threshold from mid-August to early December. Ice above the percolation threshold, combined with negative freeboard, facilitated surface flooding of the sea ice cover.

The description of the sea-ice cover presented in this paper captures much of its character as a habitat. However, even our dense thickness surveys provide only a one-dimensional point-by-point description of the ice. Under-ice video revealed regions where extensive ice rafting created an intricate habitat consisting of a three-dimensional maze of ice pieces and blocks. These regions are difficult to characterize from the surface and are potentially an important component of the under-ice habitat. More work needs to be done using divers and under-ice video to characterize this component in terms of its areal extent and morphological characteristics.

Acknowledgments

This work was funded by the National Science Foundation, Office of Polar Programs Antarctic Program. Special thanks to C. Fritsen, members of the ice sampling team, Raytheon support staff, and the crew of the R.V. *Laurence M. Gould*. We deeply appreciate the constructive and considerable contributions made by two anonymous reviewers.

References

Ackley, S.F., Sullivan, C.W., 1994. Physical controls on the development and characteristics of Antarctic sea ice biological communities—a review and synthesis. Deep-Sea Research 41, 1583–1604.

Ackley, S.F., Buck, K.R., Taguchi, S., 1979. Standing crop of algae in the sea ice of the Weddell Sea region. Deep-Sea Research 26 (3A), 269–281.

Ackley, S.F., Gow, A.J., Lytle, V.I., Darling, M.N., Yankielun, N.E., 1992. Sea ice investigations on Nathaniel B. Palmer, Cruise 92-2. Antarctic Journal of the United States 27 (5), 87–88.

Ainley, D.G., DeMaster, D.P., 1990. The upper trophic levels in polar marine ecosystems. In: Smith, W.O. (Ed.), Polar Oceanography. Stanford University. Press, San Diego, pp. 599–630.

Allison, I., Qian, S., 1985. Characteristics of sea ice in the Casey Region. ANARE Research Notes 28, 47–56.

Coplen, T.B., 1996. New guidelines for reporting hydrogen, carbon, and oxygen isotope ratio data. Geochemist Cosmochimica Acta 60, 3359–3360.

Daly, K.L., 1998. Physioecology of juvenile Antarctic krill (*Euphausia superba*) during spring in ice-covered seas. In: Lizotte, M.P., Arrigo, K.R. (Eds.), Antarctic Sea Ice: Biological Processes, Interactions and Variability. Antarctic Research Series, Washington, DC, pp. 183–198.

Eicken, H., 1992. The role of sea ice in structuring Antarctic ecosystems. Polar Biology 12, 3–13.

Eicken, H., Lange, M.A., 1989. Development and properties of sea ice in the coastal regime of the southeastern Weddell Sea. Journal of the Geophysical Research 94 (C6), 8193–8206.

Epstein, S., Mayeda, T., 1953. Variations of 18O content of waters from natural sources. Geochemist Cosmochimica Acta 4, 213–224.

Frankenstein, G.E., Garner, R., 1967. Equations for determining the brine volume of sea ice from $-0.5\,^{\circ}C$ to $-22.9\,^{\circ}C$. Journal of Glaciology 6, 943–944.

Golden, K.M., 2001. Brine percolation and the transport properties of sea ice. Annals of Glaciology 33, 28–33.

Golden, K.M., Ackley, S.F., Lytle, V.I., 1998. The percolation phase transition in sea ice. Science 282 (5397), 2238–2241.

Gow, A.J., Ackley, S.F., Weeks, W.F., Govoni, J.W., 1982. Physical and structural characteristics of Antarctic sea ice. Annals of Glaciology 3, 113–117.

Gow, A.J., Ackley, S.F., Buck, K.R., Golden, K.M., 1987. Physical and structural characteristics of Weddell Sea pack ice. CRREL Report 87–14.

Gow, A.J., Lytle, V.I., Bell, D., Ackley, S.F., 1992. Ice core studies in the western Weddell Sea. Antarctic Journal of the United States 27 (5), 89–90.

Haas, C., Thomas, D.N., Bareiss, J., 2001. Surface properties and processes of perennial Antarctic sea ice in summer. Journal of Glaciology 47 (159), 613–626.

Horner, R., Ackley, S.F., Dieckmann, G.S., Gulliksen, B., Hoshiai, T., Legendre, L., Melnikov, I.A., Reeburg, W.S., Spindler, M., Sullivan, C.W., 1992. Ecology of sea ice biota, 1, Habitat, terminology, and methodology. Polar Biology 12, 417–427.

Jacka, J.H., Allison, I., Thwaites, R., Wilson, J.C., 1987. Characteristics of the seasonal sea ice of East Antarctica and comparisons with satellite observations. Annals of Glaciology 9, 85–91.

Jeffries, M.O., Weeks, W.F., 1993. Structural characteristics and development of sea ice in the western Ross Sea. Antarctic Science 5 (1), 23–25.

Jeffries, M.O., Shaw, R.A., Morris, K., Veazey, A.L., Krouse, H.R., 1994. Crystal structure, stable isotopes ($\delta^{18}O$) and development of sea ice in the Ross, Amundsen, and Bellingshausen Seas, Antarctica. Journal of Geophysical Research 99 (C1), 985–995.

Jeffries, M.O., Li, S., Jana, R.A., Krouse, H.R., Hurst-Cushing, B., 1998. Late winter first-year ice floe thickness variability, seawater flooding and snow–ice formation in the Amundsen and Ross Seas. In: Jeffries, M.O. (Ed.), Antarctic Sea Ice: Physical Processes, Interactions and Variability. American Geophysical Union, Antarctic Research Series, Washington, DC, pp. 89–122.

Jeffries, M.O., Roy Krouse, H., Hurst-Cushing, B., Maksym, T., 2001. Snow–ice accretion and snow cover depletion on Antarctic first year sea ice floes. Annals of Glaciology 33, 51–59.

Lange, M.A., 1988. Basic properties of Antarctic sea ice as revealed by textural analysis of ice cores. Journal of Glaciology 10, 95–101.

Lange, M.A., Eicken, J., 1991. Textural characteristics of sea ice and major mechanisms of ice growth in the Weddell Sea. Annals of Glaciology 15, 210–215.

Lange, M.A., Ackley, S.F., Wadhams, P., Dieckmann, G.S., Eicken, H., 1989. Development of sea ice in the Weddell Sea, Antarctica. Annals of Glaciology 12, 92–96.

Legendre, L., Ackley, S.F., Dieckmann, G.S., Gulliksen, B., Horner, R., Hoshiai, T., Melnikov, I.A., Reeburgh, W.S., Spindler, M., Sullivan, S.W., 1992. Ecology of sea ice biota, 2, Global significance. Polar Biology 12, 429–444.

Lytle, V.I., Ackley, S.F., 1992. Snow properties and surface elevation profiles in the western Weddell Sea. Antarctic Journal of the United States 27 (5), 93–94.

Lytle, V.I., Ackley, S.F., 1996. Heat flux through sea ice in the western Weddell Sea: Convective and conductive transfer processes. Journal of Geophysical Research 101 (C4), 8853–8868.

Lytle, V.I., Ackley, S.F., 2001. Snow–ice growth: A fresh water flux inhibiting deep convection in the Weddell Sea, Antarctica. Annals of Glaciology 33, 45–50.

Marschall, H-P., 1988. The overwintering strategy of Antarctic krill under the pack-ice of the Weddell Sea. Polar Biology 9, 129–135.

Massom, R.A., Drinkwater, M.R., Haas, C., 1997. Winter snow cover on sea ice in the Weddell Sea. Journal of Geophysical Research 102 (C1), 1101–1117.

McPhee, M.G., et al., 1996. Antarctic Zone flux experiment. American Meteorological Society 77 (6), 1221–1232.

Morison, J.A., Aagaard, K., Falkner, K.K., Hatakeyama, K., Moritz, R., Overland, J.E., Perovich, D.K., Shimada, K., Steele, M., Takizawa, T., Woodgate, R., 2002. North Pole Environmental Observatory delivers early results, EOS. Transactions of the American Geophysical Union 83 (357), 360–361.

NOAA Web site, http://polar.wwb.noaa.gov/pub/ice/sh/2001/.

Palmisano, A.C., Sullivan, C.W., 1983. Sea ice microbial communities (SIMCO), 1, Distribution, abundance, and primary production of ice microalgae in McMurdo Sound, Antarctica in 1980. Polar Biology 2, 171–177.

Perovich, D.K., Elder, B., 2001. Temporal evolution and spatial variability of the temperature of Arctic sea ice. Annals of Glaciology 33, 207–212.

Quetin, L.B., Ross, R.M., 1991. Behavioral and physiological characteristics of the Antarctic krill, *Euphausia superba*. American Zoologist 31, 49–63.

Quetin, L.B., Ross, R.M., Clarke, A., 1994. Krill energetics: Seasonal and environmental aspects of the physiology of *Euphausia superba*. In: El-Sayed, S.Z. (Ed.), Southern Ocean Ecology: The BIOMASS Perspective. Cambridge University Press, Cambridge, pp. 165–184.

Quetin, L.B., Ross, R.M., Fraser, T.K., Haberman, K.L., 1996. Factors affecting distribution and abundance of zooplankton, with an emphasis on Antarctic krill *Euphausia superba*. In: Ross, R.M., Hofmann, E.E., Quetin, L.B. (Eds.), Foundations for Ecological Research West of the Antarctic Peninsula. American Geophysical Union, Antarctic Research Series, Washington, DC, pp. 357–371.

Siegel, V., Loeb, V., 1995. Recruitment of Antarctic krill *Euphausia superba* and possible causes for its variability. Marie Ecology Progress Series 123, 45–56.

Smith, R.C., Baker, K.S., Fraser, W.R., Hofmann, E.E., Karl, D.M., Klinck, J.M., Quetin, L.B., Prezelin, B.B., Ross, R.M., Trivelpiece, W.Z., Vernet, M., 1995. The Palmer LTER: A long-term ecological research program at Palmer Station, Antarctica. Oceanography 8, 77–86.

Sturm, M., Morris, K., Massom, R., 1998. Winter snow cover of the west Antarctic pack ice: Its spatial and temporal variability. In: Jeffries, M.O. (Ed.), Antarctic Sea Ice: Physical Processes, Interactions and Variability. American Geophysical Union, Antarctic Research Series, Washington, DC, pp. 89–122.

Tison, J.L., Haren, J., 1989. Isotropic, chemical, and crystallographic characteristics of first-year sea ice from Breid Bay. Antarctic Science 1, 106–125.

Trivelpiece, W.Z., Fraser, W.R., 1996. The breeding biology and distribution of Adelie Penguins: Adaptations to environmental variability. In: Ross, R.M., Hofmann, E.E., Quetin, L.B. (Eds.), Foundations for Ecological Research West of the Antarctic Peninsula. American Geophysical Union, Antarctic Research Series, Washington, DC, pp. 273–285.

Worby, A.P., 1999. Observing Antarctic Sea Ice: A Practical Guide for Conducting Sea Ice Observations from Vessels Operating in Antarctic Pack Ice. ASPECT CD-ROM.

Worby, A.P., Massom, R.A., Allison, I., Lytle, V.I., Heil, P., 1998. East Antarctic sea ice: a review of its structure, properties, and drift. In: Jeffries, M.O. (Ed.), Antarctic Sea Ice: Physical Processes, Interactions and Variability. American Geophysical Union, Antarctic Research Series, Washington, DC, pp. 41–67.